Time-Resolved Investigation of Photoinduced Birefringence in Azobenzene Side-Chain Polyester Films

Ralf Hildebrandt, Manuel Hegelich, Hans-Martin Keller, and Gerd Marowsky
Laser-Laboratorium Göttingen e.V., Hans-Adolf-Krebs-Weg 1, D-37077 Göttingen, Germany

Søren Hvilsted
Condensed Matter Physics and Chemistry Department, Risø National Laboratory, DK-4000 Roskilde, Denmark

Niels Christian Rømer Holme and P. S. Ramanujam
Optics and Fluid Dynamics Department, Risø National Laboratory, DK-4000 Roskilde, Denmark
(Received 6 July 1998)

We present time-resolved measurements of photoinduced birefringence in liquid crystalline polyester films. After excitation with a single nanosecond pulse, the induced birefringence is monitored on time scales ranging from nanoseconds up to minutes. The maximum birefringence is attained in a dark reaction after excitation. Subsequently, most of the induced birefringence is lost due to relaxation processes involving up to four different time constants. We observed that at high pulse energies the relaxation characteristics are strongly influenced by thermal effects. [S0031-9007(98)08018-1]

PACS numbers: 42.70.Df, 42.70.Ln, 61.30.Gd

Side-chain liquid crystalline polymers have received increasing attention during the last decade due to their interesting properties and their possible applications, especially in the field of optoelectronics and optical data storage [1–3]. In these materials, permanent birefringence can be both induced and erased optically. Although there have been many attempts to understand the underlying processes, no conclusive model has been proposed yet. It is supposed that the optical anisotropy is due to the statistical reorientation of the azo dye fragments perpendicular to the incident light with aggregate formation possibly being involved too [4]. The general process relies on optical induced *trans-cis* isomerization followed by thermal relaxation, giving the molecules the freedom of angular reorientation. The chromophores undergo several isomerization cycles, randomly changing their orientation. When their dipole moments become perpendicular to the polarization of the exciting light, the interaction with the light field ceases. In order to describe the time dependence of photoinduced birefringence and its relaxation, rate equations were proposed which take into account the relaxation of *cis* isomers, the orientational relaxation of the azo dye system, and the ordering time of the main-chain system [5,6].

Apart from investigations of the electronic properties on the fs time scale [7], most experiments have been performed with cw irradiation. The purpose of this paper is to demonstrate the advantages of ns-pulse excitation for the observation of molecular processes on time scales from minutes down to nanoseconds. The use of a single short pulse allows the observation of all kinds of dark reactions after the pump pulse. Furthermore, we believe that the dynamics after pulsed excitation can be quite different from those induced by a cw source, since apart from high peak intensities short pulses provide the possibility of fast thermal heating [8].

The experimental setup is shown in Fig. 1. A Nd:YAG laser pumped Optical Parametric Oscillator (Spectra Physics MOPO 710; 4 ns, 10 Hz, 420–1600 nm) served as the pump source at $\lambda_{\text{pump}} = 485$ nm, close to the absorption edge of the polyester [9]. A shutter is used to extract a single pulse. The sample is placed between crossed polarizers and continuously probed by a 5 mW Helium-Neon laser at $\lambda_{\text{probe}} = 632.8$ nm. To achieve both high time resolution and high sensitivity at the same time, our detectors are built up with amplified avalanche photodiodes (EG&G C30921E). In combination with a fast sampling oscilloscope (Tektronix TDS 620B), time resolution of 1 ns is achieved. To improve the beam profile of the pump laser, we use a homogenization unit consisting of a beam expander, two crossed arrays of 7×7 cylindrical lenses, and a collecting lens [10]. The beam profile at the surface of the sample has a rectangular shape (2 mm $\times$ 2 mm), and only the inner homogeneous

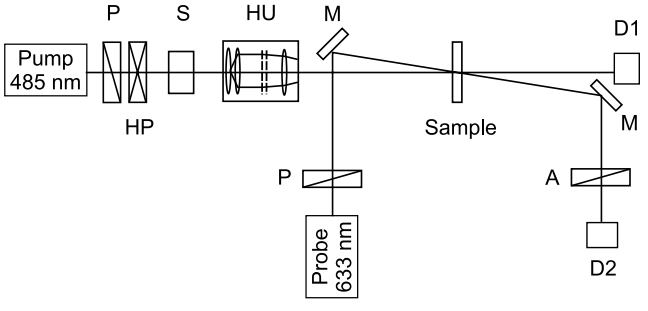

FIG. 1. Schematic diagram of the experimental setup with analyzer (A), polarizers (P), mirrors (M), detectors (D1, D2), homogenization unit (HU), half-wave plate (HP), and shutter (S). Details are explained in the text.

 0031-9007/98/81(25)/5548(4)$15.00

part is sampled by the probe beam. The linear polarization of the pump beam can be controlled by a half-wave plate and is adjusted to be at 45° relative to the probe beam.

All measurements have been performed on thin spin-coated films of poly(2-[8-[4-[(4-cyanophenyl)azo]-phenoxy]-octyl]-1,3-propylenetetradecanedioate) (P8a12) with a thickness d of about 1.8 μm at room temperature (293 K). A detailed description of the materials can be found in Hvilsted *et al.* [11]. The molecular mass characteristics with a weight average M_w of 63 000 and a number average M_n of 35 000 as determined by size exclusion chromatography renders the polyester excellent mechanical and film properties. The liquid crystalline polyester P8a12 is a polymorphic material showing up to four different organized structures [12]. The morphology strongly depends on the thermal history of the sample. By rapid cooling from the isotropic melt two nematic mesophases can be formed. Differential scanning calorimetry shows that these mesophases are metastable up to transition temperatures of 308–313 K and 319–327 K, respectively. Prolonged annealing at 311 or 331 K yields two different crystalline (or ordered smectic) phases. Only the latter is thermodynamically stable and can be directly transformed into the isotropic melt at 343 K. All the other structures are metastable and can be obtained only under nonequilibrium conditions.

Before the experiments, our sample was heated for half an hour at 350 K, which is well above the melting point at $T_c = 343$ K, and then rapidly cooled down in order to achieve an isotropic distribution of the molecules and to avoid aggregation. With $n_\perp$ and $n_\parallel$ being the components of the index of refraction perpendicular and parallel to the pump polarization, the induced birefringence $\Delta n = n_\perp - n_\parallel$ can be calculated from the measured light intensity I at the detector D2 from

$$\Delta n = \frac{\lambda_{\text{probe}}}{\pi d} \arcsin\sqrt{I/I_0}\,, \tag{1}$$

where I_0 denotes the total intensity of the probe beam before the analyzer and d is the film thickness.

We performed single pulse experiments at fluences ranging between 12 and 95 mJ/cm^2. The upper limit is determined by the single pulse ablation threshold of the film, the lower by the detection limit of the experimental setup. In order to monitor all excitation and relaxation processes covering 12 orders of magnitude from nanoseconds up to minutes, it was necessary to repeat each measurement 6 times at different sampling rates of the oscilloscope. Figure 2 is an example of such a measurement with a time resolution of 0.4 ns, showing the induced birefringence in relation to the pump pulse. Assuming similar properties of pulse and sample, the overall time dependence can be gained by the superposition of the individual data sets as shown in Fig. 3 on a logarithmic time scale for different pump fluences. A detailed look at Fig. 2 reveals that the value of birefringence strongly increases during the pump pulse. However, the maximum value is reached in a dark reaction several microseconds after the pulse involving a fast and a slow exponential increase. After that, most of the induced birefringence decreases via several relaxation processes until a relatively small permanent level is reached. We found that the data could be best fitted with a multiexponential model given by

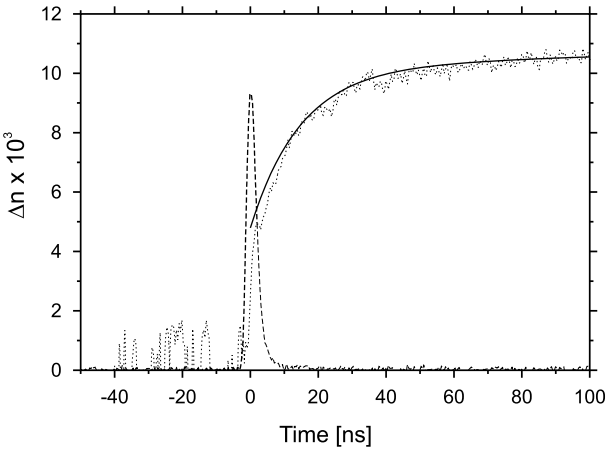

FIG. 2. Dynamics of photoinduced birefringence (dotted line) after single pulse excitation at 32 mJ/cm^2 in relation to the pump pulse (dashed line). The solid line is a multiexponential fit to the experimental data.

$$\Delta n = a_0 + \sum_{i=1}^{N} a_i\,(1 - \exp[-t/\tau_i])\,, \tag{2}$$

disregarding the first 5 ns where the pulse itself cannot be neglected. Positive values of the amplitude a_i mean an increase in birefringence, negative values characterize relaxation processes. We strictly stick to the smallest possible number of time constants yielding a good match between data and theory; a spacing of at least 1 order of magnitude between individual relaxation constants τ_i is achieved.

The fitted parameters are presented in Table I. Because of variations in film thickness, film homogeneity, and pump energy, the reproducibility is quite low leading to an error of about 30% in all absolute values. At low fluences up to 38 mJ/cm^2, two time constants for increase and four for the relaxation are necessary to describe the experimental data as shown in the lower part of Fig. 3. At higher pump fluences, however, the relaxation characteristic is changed significantly (upper part of Fig. 3). The maximum value is reached much faster involving only one time constant, and furthermore, most of the relaxation is completed within 1 μs, leaving only a small permanent value.

The induced birefringence as a function of the pump fluence is summarized in Fig. 4. The maximum value reached in the dark reaction as well as the immediate response within the pump pulse increase slightly at low fluences, but show a pronounced step between 38 and

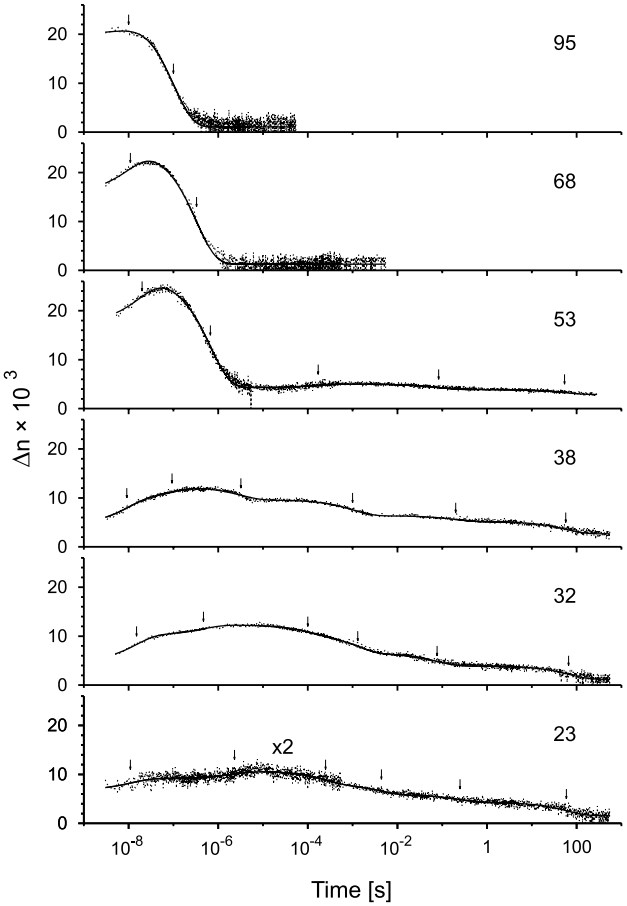

FIG. 3. Overall time dependence of the photoinduced birefringence (dotted line) on a logarithmic time scale for different fluences given on the right in mJ/cm^2. Solid lines give a multiexponential fit to the data according to Eq. (2) with the parameters listed in Table I. The arrows mark the position of the fitted time constants, each corresponding to a stepwise increase or decrease of birefringence.

56 mJ/cm^2 that corresponds to the change in relaxation characteristics described above. The permanent final value, on the other hand, shows a completely different behavior and reaches its maximum at around that threshold fluence. In general, the final value is about 1 order of magnitude smaller than the maximum value and 2 orders of magnitude smaller than the saturation level achievable in cw or multipulse exposure.

In order to explain the different behavior at low and high fluences, we have to take into account thermal effects that are induced by the pump pulse. As the mesogenic film becomes transparent after single pulse excitation at high fluences, we believe that the temperature of the film exceeds a threshold causing a transition to a glassy or amorphous phase. It is well known [8,13] that thin organic films can be heated to several hundred Kelvin by the high peak intensity of a nanosecond pulse, which is about 10 MW/cm^2 in our experiments. Therefore we assume that for high fluences above 38 mJ/cm^2, the polymer film remains in an isotropic, maybe metastable phase for a short period of time, before the thermal energy deposited in the film is conducted into the substrate. In addition, the mobility of the molecules strongly depends on temperature, though thermal effects should be considered even at lower pulse energies in contrast to cw investigations. In Ref. [13], possible interactions of the light pulse and a polymeric medium are discussed such as absorption of light in activated stages, rapid radiative and nonradiative decay processes, internal conversion of light to heat, and intrinsically slower processes such as thermally induced melting and flow.

During the pulse, molecules with their azo groups lying parallel to the pump polarization are both electronically and vibrationally excited, leading to an anisotropic orientation distribution of the ground state *trans* molecules and an instantaneous increase of birefringence. In the following, the statistical reorientation of the excited molecules as well as aggregate formation or main-chain ordering may cause a further increase (dark reaction). The higher the fluence and thus the increase in temperature, the higher is the mobility of the system. This is confirmed by both the increase of the maximum birefringence reached in the dark reaction and the decrease of the time constants in Table I for increasing fluences. However, a high mobility supports also the relaxation of aligned molecules resulting in a rapid growth of disorder in the system and the lack of permanent birefringence. As a consequence, medium intensities heating the sample close to the phase

TABLE I. Fit parameters retrieved from the multiexponential fit of the data presented in Fig. 3. Note that 1.1-8 is an abbreviation for 1.1×10^{-8}, and all amplitudes a_i have to be multiplied by 10^{-3}.

	Fluence [mJ/cm^2]											
	23		32		38		53		68		95	
i	a_i	τ_i	a_i	τ_i	a_i	τ_i	a_i	τ_i	a_i	τ_i	a_i	τ_i
0	3.4		4.8		4.5		17.5		15.9		19.9	
1	1.2	1.1-8	5.4	1.5-8	5.0	9.1-9	9.4	2.0-8	9.1	1.1-8	4.6	1.0-8
2	0.8	2.3-6	2.1	4.7-7	2.7	9.3-8	−22.7	6.7-7	−23.8	3.3-7	−23.5	1.0-7
3	−1.3	2.5-4	−1.8	1.0-4	−2.7	3.2-6	0.7	1.7-4				
4	−1.1	4.4-3	−4.0	1.3-3	−3.2	1.0-3						
5	−0.8	2.5-1	−2.6	7.7-2	−1.2	2.0-1	−1.1	8.3-2				
6	−1.4	59	−2.7	66	−2.5	57	−1.0	54				

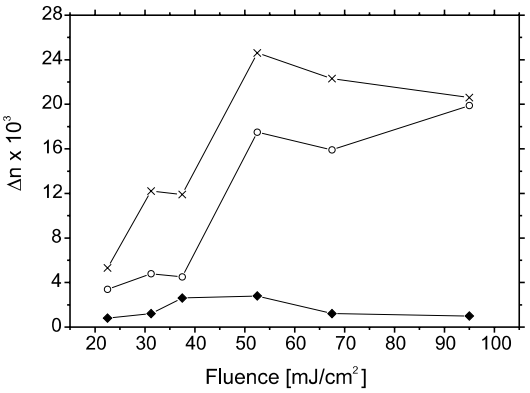

FIG. 4. Induced birefringence Δn for various fluences. Diamonds show the permanent values after relaxation, open circles the immediate response during the pulse, and crosses denote the maximum value reached during dark reaction.

transition as described above are best for both inducing and preserving birefringence. This corresponds with the results obtained in cw exposure which also showed that a maximum value of permanent birefringence can only be reached close to the glass transition [14].

To investigate the physical meaning of the various relaxation time constants, we performed measurements with a sample heated over the melting point T_c and a solution of the polymer in toluene. Both experiments showed no detectable change in birefringence over the entire time scale. The mobility of the molecules seems to be so high that any anisotropic intensity distribution is disturbed instantaneously. To check the influences of the liquid crystalline mesophases present in P8a12, we performed measurements with a polyester, P6aP, where the same azobenzene moiety is linked through a hexamethylene spacer to the main chain in which the tetradecanedioate is replaced by the aromatic phthalate. This polyester is amorphous with a T_g at 316 K. We found nearly the same relaxation characteristics, leading to the conclusion that the mesophases do not influence the process strongly. Therefore vibronic relaxation processes or the decay of long living triplet states may be responsible for the complex nature of the decay of birefringence.

Even though we cannot assign a detailed physical process to any of the time constants at the moment, the experiments presented here give important information about the dynamics of photoinduced birefringence using pulsed pump sources. We monitored for the first time the relaxation behavior of the induced birefringence which reveals a number of time constants depending on the pump energy. Major consequences of our investigations are that in contrast to cw exposure, thermal effects originating from the pump pulse cannot be neglected, and that a permanent value of birefringence can be best induced at medium pump energies causing moderate heating of the sample. Furthermore, the fact that permanent birefringence can be induced by a single nanosecond pulse might be important for applications in optical data storage.

We thank V. Westphal for the implementation of the beam homogenization unit and J. Jethwa for helpful comments. Support by the COST action 518 "Molecular Materials and Functional Polymers for Advanced Devices" of the European Commission is also gratefully acknowledged.

[1] *Side Chain Liquid Crystal Polymers*, edited by C. B. McArdle (Blackie and Son Ltd., Glasgow, 1989), Chap. 13, pp. 357–394 (and cited literature).
[2] M. Eich and J. H. Wendorff, J. Opt. Soc. Am. B **7**, 1428 (1990).
[3] *Special Polymers for Electronics and Optoelectronics*, edited by J. A. Chilton and M. T. Gossey (Chapman and Hall, London, 1995).
[4] K. Anderle, R. Birenheide, M. Eich, and J. H. Wendorff, Makromol. Chem. Rapid Commun. **10**, 477 (1989).
[5] T. G. Pedersen, P. M. Johansen, N. C. R. Holme, P. S. Ramanujam, and S. Hvilsted, J. Opt. Soc. Am. B **15**, 1120 (1998).
[6] C. Kulinna, S. Hvilsted, C. Hendann, H. W. Siesler, and P. S. Ramanujam, Macromolecules **31**, 2141 (1998).
[7] N. C. R. Holme, T. B. Norris, M. Pedersen, S. Hvilsted, and P. S. Ramanujam, Polym. Prepr. **39**, 334 (1998).
[8] K. E. Evans, J. Appl. Phys. **63**, 4946 (1988).
[9] S. Hvilsted, F. Andruzzi, and P. S. Ramanujam, Opt. Lett. **17**, 1234 (1992).
[10] K. Mann, J. Ohlenbusch, and V. Westphal, Laser Optoelektron. **30**, 66 (1998).
[11] S. Hvilsted, F. Andruzzi, C. Kulinna, H. W. Siesler, and P. S. Ramanujam, Macromolecules **28**, 2172 (1995).
[12] E. L. Tassi, M. Paci, and P. L. Magagnini, Mol. Cryst. Liq. Cryst. **266**, 135 (1995).
[13] B. J. Bartholomeusz, Appl. Opt. **31**, 909 (1992).
[14] N. C. R. Holme, P. S. Ramanujam, and S. Hvilsted, Appl. Opt. **35**, 4622 (1996).